Published in final edited form as:

J Am Chem Soc. 2022 October 19; 144(41): 18876–18886. doi:10.1021/jacs.2c05565.

Characterization of a Radical SAM Oxygenase for the Ether Crosslinking in Darobactin Biosynthesis

Hai Nguyen,
Department of Biochemistry, Duke University School of Medicine, Durham, North Carolina 27710, United States

I Dewa Made Kresna,
Institute for Insect Biotechnology, Justus-Liebig-University of Giessen, 35392 Giessen, Germany

Nils Böhringer,
Institute for Insect Biotechnology, Justus-Liebig-University of Giessen, 35392 Giessen, Germany; German Center for Infection Research (DZIF), Partner Site Giessen-Marburg-Langen, 35392 Giessen, Germany

Jeremie Ruel,
University of Grenoble Alpes, CEA, CNRS, IBS, Metalloproteins Unit, F-38000 Grenoble, France

Eugenio de la Mora,
University of Grenoble Alpes, CEA, CNRS, IBS, Metalloproteins Unit, F-38000 Grenoble, France

Jil-Christine Kramer,
Institute for Insect Biotechnology, Justus-Liebig-University of Giessen, 35392 Giessen, Germany

Kim Lewis,
Antimicrobial Discovery Center, Department of Biology, Northeastern University, Boston, Massachusetts 02115, United States

Yvain Nicolet,
University of Grenoble Alpes, CEA, CNRS, IBS, Metalloproteins Unit, F-38000 Grenoble, France

Till F. Schäberle,
Institute for Insect Biotechnology, Justus-Liebig-University of Giessen, 35392 Giessen, Germany; German Center for Infection Research (DZIF), Partner Site Giessen-Marburg-Langen, 35392

Corresponding Authors Yvain Nicolet – University of Grenoble Alpes, CEA, CNRS, IBS, Metalloproteins Unit, F-38000 Grenoble, France; yvain.nicolet@ibs.fr; **Till F. Schäberle** – Institute for Insect Biotechnology, Justus-Liebig-University of Giessen, 35392 Giessen, Germany; German Center for Infection Research (DZIF), Partner Site Giessen-Marburg-Langen, 35392 Giessen, Germany; Department of Bioresources, Fraunhofer Institute for Molecular Biology and Applied Ecology, 35392 Giessen, Germany; Till.F.Schaeberle@agrar.uni-giessen.de; **Kenichi Yokoyama** – Department of Biochemistry, Duke University School of Medicine, Durham, North Carolina 27710, United States; Department of Chemistry, Duke University, Durham, North Carolina 27710, United States; ken.yoko@duke.edu.

Author Contributions

The manuscript was written through contributions of all authors. All authors have given approval to the final version of the manuscript.

The authors declare no competing financial interest.

Supporting Information

The Supporting Information is available free of charge at https://pubs.acs.org/doi/10.1021/jacs.2c05565.

Oligo sequence; sodium dodecyl sulfate polyacrylamide gel electrophoresis and UV–vis spectra of DarA and DarE; MS and MS/MS spectra of DarA, modified DarA, proteolyzed DarE products, darobactin A; and 5′-dA; and AlphaFold model of DarE (PDF)

Giessen, Germany; Department of Bioresources, Fraunhofer Institute for Molecular Biology and Applied Ecology, 35392 Giessen, Germany

Kenichi Yokoyama

Department of Biochemistry, Duke University School of Medicine, Durham, North Carolina 27710, United States; Department of Chemistry, Duke University, Durham, North Carolina 27710, United States

Abstract

Darobactin A is a ribosomally synthesized, post-translationally modified peptide (RiPP) with potent and broad-spectrum anti-Gram-negative antibiotic activity. The structure of darobactin A is characterized by an ether and C–C crosslinking. However, the specific mechanism of the crosslink formation, especially the ether crosslink, remains elusive. Here, using in vitro enzyme assays, we demonstrate that both crosslinks are formed by the DarE radical *S*-adenosylmethionine (SAM) enzyme in an O_2-dependent manner. The relevance of the observed activity to darobactin A biosynthesis was demonstrated by proteolytic transformation of the DarE product into darobactin A. Furthermore, DarE assays in the presence of $^{18}O_2$ or [^{18}O]water demonstrated that the oxygen of the ether crosslink originates from O_2 and not from water. These results demonstrate that DarE is a radical SAM enzyme that uses oxygen as a co-substrate in its physiologically relevant function. Since radical SAM enzymes are generally considered to function under anaerobic environments, the discovery of a radical SAM oxygenase represents a significant change in the paradigm and suggests that these radical SAM enzymes function in aerobic cells. Also, the study revealed that DarE catalyzes the formation of three distinct modifications on DarA; ether and C–C crosslinks and *α,β*-desaturation. Based on these observations, possible mechanisms of the DarE-catalyzed reactions are discussed.

Graphical Abstract

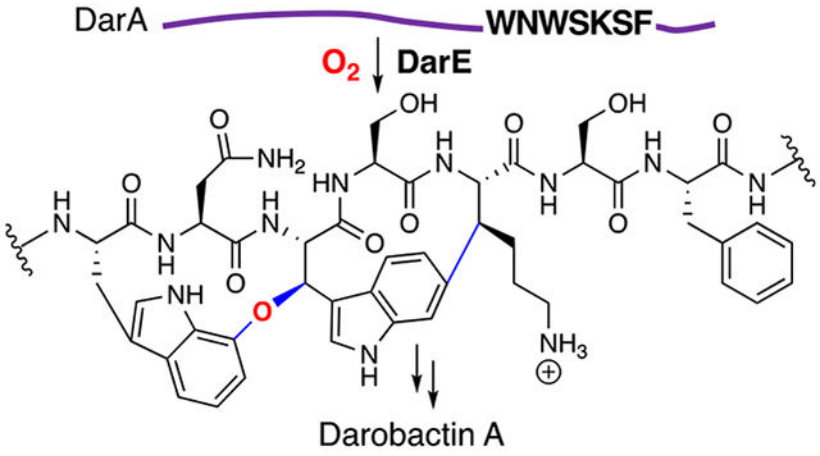

INTRODUCTION

The bicyclic heptapeptide darobactin A is a ribosomally synthesized, post-translationally modified peptide (RiPP) with antibiotic activities against diverse sets of Gram-negative

bacteria including many clinically important pathogens.[1] Darobactin A exhibits its antibiotic activity by inhibiting BamA, a protein in the Bam complex responsible for the assembly of proteins in the outer membrane of Gram-negative bacteria.[1,2] Darobactin A has a rigid β-strand conformation through the ether and C–C crosslinks on the heptapeptide core structure (W^1–N^2–W^3–S^4–K^5–S^6–F^7, see Figure 1 for the structure), which mimics the recognition signal of native substrates and blocks the open lateral gate of BamA.[2] However, the mechanism by which this unique and biologically important bicyclic structure is formed remains unknown.

The darobactin biosynthetic gene cluster (BGC) consists of the precursor peptide-encoding *darA*, the transporter genes *darBCD*, and a radical *S*-adenosyl-L-methionine (SAM) enzyme gene *darE* (Figure 1a). Earlier studies have established that the co-expression of DarA and DarE is sufficient for the production of darobactin A in *Escherichia coli*[1,3,4] (Figure 1b). Radical SAM enzymes form a large enzyme superfamily[5] and catalyze various radical-mediated reactions.[6] These enzymes harbor an oxygen-sensitive 4Fe–4S cluster to catalyze the reductive cleavage of SAM to transiently generate the 5′-deoxyadenosyl radical (5′-dA•) that then in most cases abstracts a H atom from the substrate or, in other cases, adds to the substrate to carry out various radical reactions. Since the 4Fe–4S clusters of radical SAM enzymes are oxygen-sensitive, characterization of these enzymes has been performed under strictly anaerobic conditions, and it has been largely assumed that these enzymes must function in the absence of oxygen. So far, no radical SAM enzymes have been reported to have physiological functions that require molecular oxygen as the co-substrate.

In the past decade, many radical SAM enzymes have been identified to be responsible for the maturation of RiPPs. In particular, radical SAM enzymes in the SPASM subfamily,[7] characterized by the presence of auxiliary 4Fe–4S clusters (AUX) in addition to the canonical radical SAM 4Fe–4S cluster, were reported to catalyze the formation of various crosslinks during RiPP biosynthesis. Such crosslinks include C–C bonds between aromatic and aliphatic carbons,[8,9] thioethers via a Cys residue,[10] and an ether via Thr alcohol.[11] However, all of these reported crosslinks utilize functional groups already available in the precursor peptides. In contrast, the ether ring in darobactin A is unique in that the oxygen atom of the ether must be post-translationally installed. The origin of this oxygen atom and the mechanism of its installation remain ambiguous.

Recently, when this manuscript was in preparation, Guo et al. reported in vitro characterization of *Photorhabdus khanii* DarE with an N-terminal His-tag.[12] The authors reported the formation of DarA with an ether crosslink without the C–C crosslink as the major product and proposed water as the source of the ether oxygen. However, no evidence was provided for whether such a compound may be converted into darobactin A, and hence, the biological relevance of this observation remained unclear.

Here, we report the successful in vitro reconstitution of darobactin A biosynthesis. Importantly, our ^{18}O-labeling study provides strong evidence that the oxygen atom of the ether crosslink is derived from molecular oxygen and not from water, making DarE the first radical SAM oxygenase. These results extend the repertoire of the reactions catalyzed

by radical SAM enzymes and provide the evidence for their function under an aerobic environment.

MATERIALS AND METHODS

General.

Sodium dithionite (SDT) was purchased from Sigma-Aldrich. β-Mercaptoethanol (βME) was obtained from Calbiochem. Dithiothreitol (DTT) was obtained from Amresco. G-25 Sephadex resin was obtained from GE Healthcare. Ni-NTA agarose resin was obtained from Qiagen. Strep-Tactin XT 4Flow high-capacity resin was obtained from IBA LifeSciences. *E. coli* DH5α and BL21(DE3) competent cells were obtained from Invitrogen. All anaerobic experiments were carried out in an MBRAUN glovebox maintained at 10 ± 2 °C with an O_2 concentration of <0.1 ppm. All anaerobic buffers were degassed on a Schlenk line and equilibrated in the glovebox overnight. All plastic devices were evacuated in the antechamber of the glovebox overnight before use. All high-performance liquid chromatography (HPLC) experiments were performed on a Hitachi L-2130 pump equipped with an L-2455 diode array detector, an L-2485 fluorescence detector, an L-2200 autosampler, and an L-2300 column oven maintained at 40 °C. UV–vis absorption spectra were determined using a U-3900 UV–vis ratio recording double-beam spectrometer (Hitachi). All mass spectra were recorded on a 6224 accurate-mass time-of-flight mass spectrometer (Agilent) equipped with a Dual ESI source, and accurate mass data were obtained by internal calibration using a secondary nebulizer to continuously deliver the reference solution. Liquid chromatography mass spectrometry (LC–MS) analysis was conducted on a 6224 TOF LC/MS system equipped with a Phenomenex Kinetex C18 EVO column (3 × 100 mm, 2.6 μm particle), monitored by a diode array detector (254 nm). Chromatography was performed with the flow rate of 0.5 mL/min using solvents A (H_2O/MeOH/formic acid = 100:3:0.3) and B (H_2O/MeCN/formic acid = 3:100:0.3) and the following gradient conditions: 100% A isocratic between 0 and 0.5 min and 0–50% B linear gradient between 0.5 and 8 min.

Heterologous Production of Darobactin A.

The *Pseudoalteromonas luteoviolacea darA* and *darE* genes were codon optimized for *E. coli* using the Java Codon Adjustment Tool (jCAT),[13] and the resulting sequences were synthesized by Eurofins Genomics (Eberswalde, Germany). The resulting synthetic *darA* and *darE* genes were PCR amplified using the primer pairs darA-f/darA-r and darE-f/darE-r (Table S1) using Q5 polymerase (NEB Biolabs, New Brunswick, USA) according to the manufacturer's manual. All PCR products were gel purified using 1 or 2% TAE agarose gels, and DNA was recovered using the Zymo Research Large Fragment DNA Recovery Kit (Zymo Research, USA) according to the manufacturer's manual. An empty pRSFduet-1 plasmid (Novagen) was digested using *Nde*I/*Avr*II. All fragments were assembled using a homemade isothermal assembly master mix,[14] and the assembled plasmids were transferred to *E. coli* Top10 using the standard electroporation methodology and selected on LB_{Kan}. The identity of the plasmids was corroborated by test restriction. The correctly assembled plasmid was transferred to *E. coli* Bap1 and *E. coli* Bap1 harboring pGro7 (Takara) by electroporation. *E. coli* Bap1 + pRSFduet-1 (empty vector) was used as a negative control.

For heterologous Darobactin production, 20 mL of LB_{Kan} was inoculated with an overnight preculture of *E. coli* Bap1 + pRSFduet-1, *E. coli* Bap1 + pRSF-darAE$_{Pse}$ of *E. coli* Bap1 + pRSF-darAE$_{Pse}$ + pGro7 (Takara) cells, and the cultures were incubated at 30 °C to an OD_{600} of ~0.5. Transcription was induced by the addition of isopropyl β-D-1-thiogalactopyranoside (IPTG) to a 1 mM final concentration. After 3 days of cultivation, 0.5 mL of the culture was separated into the supernatant and pellet by centrifugation, and the cleared supernatant was applied to self-packed C18 stage tips. The stage tips were washed using ddH_2O, the material was eluted in 50 μL of 80:20 MeCN/H_2O, and 5 μL of the concentrated supernatants were analyzed by LC–MS using a 20 μg/mL darobactin A solution as the standard.

Expression and Purification of *Pl*DarA.

The *P. luteoviolacea darA* gene with the His_6- and SUMO-tags fused at its 5′-end was synthesized using Genscript with the codon usage optimized for *E. coli* and cloned into the *Nco*I-*Bam*HI site of pET16b (pET16b-SUMO-*Pl*DarA). *Pl*DarA was then expressed in *E. coli* BL21(DE3) cells harboring pET16b-SUMO-*Pl*DarA and pGro7. The *E. coli* cells were grown in LB medium (50 mL) with 100 mg/L ampicillin and 30 mg/L chloramphenicol and incubated at 37 °C, 220 rpm overnight until saturation. An aliquot (30 mL) of the overnight culture then was used to inoculate 1.5 L of LB medium with the same antibiotics, which was grown at 37 °C, 220 rpm until OD_{600} = 0.6–0.8. Protein expression was induced with 60 mg/L IPTG, and the culture was incubated at 18 °C, 220 rpm for 20 h. The cells were harvested by centrifugation, washed with buffer A (50 mM Tris–HCl pH 7.6, 150 mM NaCl, 10% v/v glycerol), frozen with liquid nitrogen, and stored at −20 °C. Approximately 6.1 g of the wet cell paste was obtained per liter of the culture.

SUMO-*Pl*DarA Purification.

In a typical purification, 20 g of the cell pellet was suspended and homogenized in 80 mL of buffer A supplemented with 5 mM β-ME and 0.8 mL of a protease inhibitor cocktail (100X ProteaseArrest, G-Biosciences). The cell suspension was lysed by two passages through a French pressure cell operating at 14,000 psi. The resulting lysate was cleared by centrifugation (20,000×*g*, 20 min, 4 °C). The supernatant was incubated with Ni-NTA agarose resin (Qiagen, 10 mL equilibrated in buffer A containing 20 mM imidazole and 1.0 μl benzonase/30 mL supernatant) for 1 h. The resin was washed with 10 volumes of buffer A with 20 mM imidazole and 3 mM β-ME, and the protein was eluted with buffer A with 400 mM imidazole and 3 mM β-ME. Fractions containing SUMO-*Pl*DarA were exchanged into buffer A using a Sephadex G-25 column. The concentration of SUMO-*Pl*DarA was determined by the Bradford assay using bovine serum albumin (BSA) as a standard. The resultant protein solution was frozen in liquid N_2 and stored at −80 °C. Typically, 14 mg of SUMO-*Pl*DarA was prepared from each gram of the wet cell paste. The SUMO tag of SUMO-*Pl*DarA (100 mg) was cleaved by SUMO-protease (0.3 mg) at 0 °C for 1 h. The resulting solution was passed through Ni-NTA agarose resin (10 ml equilibrated in distilled water). The protein was eluted with distilled water. Fractions containing *Pl*DarA were brought into an mBraun anaerobic glovebox ([O_2] < 0.1 ppm) and exchanged into anaerobic water using a Sephadex G-25 column. The concentration of *Pl*DarA was determined by HPLC.

Expression of His-*Pl*DarE.

pRSF-His-*Pl*DarE was created by amplifying $darE_{Pse}$ using the primers his-darE-f/his-darE-r (Table S1) using Q5 polymerase (NEB) according to the manufacturer's manual. The amplified gene was gel purified using 1% TAE agarose gels and the ZymoResearch Large Fragment DNA Recovery Kit according to the manufacturer's manual. The purified fragment was then digested with *Bam*HI/*Sal*I and cloned into the corresponding site of pRSFduet-1. Both fragments were fused using a homemade isothermal assembly master mix,[14] transferred to *E. coli* Top10 using the standard electroporation methodology, and selected on LB_{Kan}. The correct assembly was verified by sequencing, and the plasmid was designated as pRSF-His-*Pl*DarE. To express His-*Pl*DarE, *E. coli* Bap1 cells were transformed with pRSF-His-*Pl*DarE and pGro7. The resulting transformant was grown in LB medium (50 mL) with 50 mg/L kanamycin and 30 mg/L chloramphenicol and incubated at 37 °C, 220 rpm overnight until saturation. An aliquot (30 mL) of the overnight culture was then used to inoculate 1.5 L of terrific broth containing 50 mg/L cysteine, 30 mg/L iron(III), and 0.5 g/L L-arabinose with the same antibiotics, which was grown at 37 °C, 220 rpm until OD_{600} = 0.6–0.8. Protein expression was induced with 60 mg/L IPTG, and the culture was incubated at 18 °C, 220 rpm for 20 h. The cells were harvested by centrifugation, washed with buffer A (50 mM Tris pH 7.6, 150 mM NaCl, 10% glycerol), frozen with liquid nitrogen, and stored at −20 °C. Approximately 22 g of the wet cell paste was obtained per liter of the culture.

Purification of His-*Pl*DarE.

His-*Pl*DarE was anaerobically purified typically from 10–30 g of the cell paste of *E. coli* BAP1 harboring pRSF-His-*Pl*DarE. The cell pellet was brought into an mBraun anaerobic glovebox ($[O_2]$ < 0.1 ppm). Then, each gram of the cell pellet was suspended and homogenized in 4 mL of anaerobic buffer A supplemented with 5 mM β-ME. The cell suspension was brought out of the glovebox and lysed by two passages through a French pressure cell operating at 14,000 psi under a constant Ar flow. The resulting lysate was cleared by centrifugation (20,000×*g*, 20 min, 4 °C) using centrifugal tubes filled with Ar gas and brought back to the glovebox. All subsequent purification steps were carried out under strict anaerobic conditions in the glovebox ($[O_2]$ < 0.1 ppm) maintained at 10 °C. The dark brown-colored supernatant was incubated with Ni-NTA agarose resin (Qiagen, 20 mL equilibrated in buffer A containing 40 mM imidazole and 1.0 μL benzonase/30 mL supernatant) for 1 h. The resin was washed with 10 volumes of buffer A with 20 mM imidazole and 3 mM β-ME, and the protein was eluted with buffer A with 400 mM imidazole and 3 mM β-ME. Fractions containing dark brown-colored His-*Pl*DarE were exchanged into buffer A using a Sephadex G-25 column. The concentration of His-*Pl*DarE was determined by the Bradford assay using BSA as a standard. The amounts of $Fe^{2+/3+}$ were quantified by the following published protocols.[15] Typically, the preparation yielded His-*Pl*DarE with 4.0 ± 0.8 Fe per monomer. The resulting purified His-*Pl*DarEwas immediately used for anaerobic reconstitution carried out at 10 °C by a slow addition of 8–12 equiv $Fe^{II}(NH_4)_2(SO_4)_2$ and Na_2S per His-*Pl*DarE monomer over the course of 10 min. The amounts of $Fe^{II}(NH_4)_2(SO_4)_2$ and Na_2S were adjusted based on the amounts of $Fe^{2+/3+}$ associated with the as-isolated His-*Pl*DarE. The resulting mixture was incubated for 60 min at 10 °C. The protein was then desalted using a Sephadex G-25 column equilibrated

with buffer A. The amounts of Fe and sulfide were determined by the ferrozine assay.[15] The resultant protein solution was frozen in liquid N_2 and stored at −80 °C. Typically, 0.8 mg of His-*Pl*DarE was prepared from each gram of the wet cell paste.

Expression and Purification of Untagged *Pl*DarE.

The Twin-strep II tag and the Factor Xa cleavage site (MASAWSHPQ-FEKGGGSGGGSGGSAWSHPQFEKSGIEGR) were introduced to the 5′-end of the codon optimized *P. luteoviolacea darE* gene by PCR. The pRSF-His-*Pl*DarE plasmid was amplified using a primer pair pRSF-strep-DarE-f/r (Table S1) and ligated with a strep-f/r oligo pair (Table S1) using the InFusion kit (Takara). The resulting plasmid pRSF-Strep-*Pl*DarE was then used as a template to amplify the Strep-*Pl*DarE gene using a primer pair pET-strep-*Pl*DarE-f/r (Table S1). The resulting PCR products were digested with *Nde*I and *Hin*dIII and introduced into the corresponding site of pET30b to yield pET30-Strep-*Pl*DarE. Strep-*Pl*DarE was expressed in an identical way to His-*Pl*DarE using *E. coli* Bap1 with pET30-Strep-*Pl*DarE and pGro7. Approximately 6.9 g of the wet cell paste was obtained per liter of the culture. To purify Strep-*Pl*DarE, the *E. coli* cells were lysed in the same manner as that for His-*Pl*DarE. The cleared lysate was loaded onto the Strep-Tactin XT 4Flow high-capacity resin, the column was washed with 10 column volumes of buffer W (100 mM Tris–HCl pH 8.0, 150 mM NaCl), and the protein was eluted with buffer BXT (100 mM Tris–HCl pH 8.0, 150 mM NaCl, and 50 mM biotin). Fractions containing dark brown-colored *Pl*DarE were exchanged into buffer W using a Sephadex G-25 column. The concentration of *Pl*DarE was determined by the Bradford assay using BSA as a standard. The strep tag was removed by incubation with Factor Xa protease (1 μg per 1 mg protein, New England Biolabs) in buffer W supplemented with 2 mM $CaCl_2$ at 10 °C for 4 h. Then, the Factor Xa protease was removed by Xarrest resin, and the cleaved strep tag was removed using Strep-tactin resin. The 4Fe–4S cluster was reconstituted as described above for His-*Pl*DarE, and the resulting reconstituted *Pl*DarE contained 12.2 ± 0.5 Fe per monomer. Typically, 2.0 mg of *Pl*DarE was prepared from each gram of the wet cell paste.

DarE Activity Assay.

His-*Pl*DarE or *Pl*DarE (50 μM) was anaerobically incubated with DarA (50 μM) in the presence of SAM (1.0 mM), flavodoxin (10 μM), flavodoxin reductase (2.0 μM), NAD(P)H (1.0 mM), and oxygen (100 μM) in an airtight glass vial with a total volume of 50 μL of buffer H (20 mM HEPES pH 8.0) supplemented with 5 mM DTT for 3 h at 25 °C. The reaction was initiated by adding DarA and oxygen-saturated buffer H. After 3 h of incubation, the reaction was diluted twice and boil-quenched at 100 °C for 5 min. After the removal of the precipitate by centrifugation, an aliquot (40 μL) of the supernatant was injected into the HPLC system equipped with an XSelect Peptide CSH C18 column (Waters) equilibrated in 0.1% trifluoroacetic acid (TFA) in water. The elution was achieved with a flow rate at 1.0 mL/min using solvents A (0.1% TFA in water) and B (0.1% TFA in MeCN): 3% B for 5 min, 3–27% B for 5–15 min, and 27–30% B for 15–50 min. Chromatography was performed using the L-2455 diode array detector.

Purification of DarE Products.

A DarE reaction (1.0 ml) was performed in the conditions described above and quenched with 1 ml of buffer Q (0.2% TFA and 6% MeCN in water). After the removal of the precipitate by centrifugation, an aliquot (500 μL) of the supernatant was injected into the HPLC system and chromatographed under the above-mentioned conditions. P1 and P2 were monitored using the L-2455 diode array detector and eluted at 44 and 30 min, respectively. After combining all the fractions containing P1 or P2, TFA and MeCN were removed using a centrifugal evaporator. The resulting solution was lyophilized and redissolved in water. HRMS (ESI-TOF): *m/z* calcd for P1, $C_{281}H_{448}N_{74}O_{89}$, $[M+7H]^{+7}$, $^{13}C = 3$) 899.0493; found, 899.0417; *m/z* calcd for P2, ($C_{281}H_{446}N_{74}O_{90}$, $[M+7H]^{+7}$, $^{13}C = 4$) 901.1897; found, 901.1809.

Proteinase K Treatment of DarE Products.

P1 and P2 (2.5 μg) were treated with proteinase K (100 ng) in 20 μL ofbuffer K (50 mM Tris–HCl pH 8.0 and 5.0 mM $CaCl_2$) for 1 h at 37 °C. The reaction mixture was then quenched with an equal volume of buffer Q. Precipitation was removed, and an aliquot (20 μL) of the supernatant was analyzed by HPLC. Another aliquot (5 μL) was analyzed by LC–high-resolution MS (LC–HRMS). HRMS (ESI-TOF): *m/z* calcd for proteinase K-digested P1, ($C_{35}H_{43}N_9O_8$, $z = +2$) 359.6696; found, 359.6689; *m/z* calcd for proteinase K-digested P2, ($C_{47}H_{55}N_{11}O_{12}$, $z = +2$) 483.7094; found, 483.7097.

$^{18}O_2$ Incorporation Experiments.

$^{18}O_2$-saturated buffer H was prepared by degassing buffer H on a Schlenck line followed by a refill with $^{18}O_2$ gas (97% enrichment, Cambridge Isotope Laboratory). *Pl*DarE assays with $^{18}O_2$ were performed in a way identical to the assays described above, except that an aliquot (10 μL) of each reaction mixture was added to proteinase K (100 ng) and buffer K (40 μL). The resulting solution was incubated at 37 °C for 1 h and subsequently centrifuged to collect the supernatant for LC–MS analysis.

$H_2{}^{18}O$ Incorporation Experiments.

The *Pl*DarE assay (0.5 mL) with $H_2{}^{18}O$ was performed as described above, except that HEPES buffer was prepared in 95% ^{18}O enriched water. The final ^{18}O enrichment in the assay mixture was ~80%. P2 was purified by HPLC and characterized as described above.

P1, P2, and 5′-dA Quantitation.

DarE assays (60 μL) were performed in the conditions described above and diluted twice with distilled water followed by boil-quenching at 100 °C for 5 min. After the removal of the precipitate by centrifugation, an aliquot (60 μL) of the supernatant was analyzed by HPLC under the above-mentioned conditions. The elution was monitored by absorption at 280 nm, and P1 and P2 were eluted at 50 and 36 min, respectively. P1 was quantified by comparing the peak areas with that of a synthetic DarA core peptide (WNWSKSF, purchased from Genscript, $\varepsilon_{280\ nm} = 11.2\ mM^{-1}\ cm^{-1}$). The concentration of P2 was determined using darobactin A as a standard. The concentration of darobactin A was determined by NMR in the presence of a known concentration of benzaldehyde as an internal standard. 5′-dA

was quantified by analyzing the same supernatant (10 μL) using HPLC equipped with an XSelect Peptide CSH C18 column (Waters) equilibrated in 30 mM ammonium formate buffer pH 4.0 (solvent C). The elution was performed with a flow rate at 0.5 mL/min using solvent C and methanol (solvent D): 1–60% D for 0–15 min and 60–99% B for 15–16 min. Chromatography was performed at 260 nm. The concentration of 5′-dA was determined by comparing the peak areas with those of the 5′-dA standard (Sigma, $\varepsilon_{259\ nm}$ = 15.4 $mM^{-1}\ cm^{-1}$). The reported quantitation was an average of six repeats, and the errors are the standard deviation.

RESULTS

In search for the soluble expression in *E. coll*, we screened several DarEs from different organisms and identified that DarE from *P. luteoviolacea* (*Pl*DarE) can be expressed as a soluble protein. When *Pl*DarE was co-expressed with *P. luteoviolacea* DarA (*Pl*DarA) in *E. coli*, darobactin A production was observed (Figure S1a). The identity of darobactin A was confirmed based on the LC–MS comparison with the structurally characterized darobactin A standard (Figure S1).

Based on the observation in *E. coli*, we expressed and purified *Pl*DarE in *E. coli*. Initially, we used N-terminally His_6-tagged *Pl*DarE (His-*Pl*DarE) that was purified to >90% purity (Figure S2) with the broad light absorption feature characteristic for 4Fe–4S cluster proteins (Figure S3). The as-isolated His-*Pl*DarE had 3.6 ± 0.9 Fe per monomer, which was increased to 8.8 ± 0.3 Fe per monomer after chemical reconstitution of the cluster. Since DarE is a member of the SPASM subfamily with conserved Cys ligands for the three 4Fe–4S clusters, supported by sequence alignment (Figure S4) and an AlphaFold structural prediction (Figure S5), the theoretical Fe content of the fully loaded DarE is 12 per monomer. Thus, the observed amount of Fe likely represents only partial loading of the three clusters.

The catalytic function of His-*Pl*DarE was assessed using recombinant *Pl*DarA. To this end, we expressed *Pl*DarA in *E. coli* as an *N*-terminal fusion with the His_6-tag and a SUMO protein. After purification using a Ni-NTA column, the His-SUMO tag was removed by treating with the SUMO protease to prepare the full-length and untagged DarA The identity of the purified DarA was confirmed by LC–MS (Figure S6). When the purified DarA was incubated with His-*Pl*DarE under anaerobic conditions in the presence of SAM and the flavodoxin system as a reductant, we observed the formation of a product (P0, Figure 2a). This compound exhibited a UV–vis absorption spectrum similar to that of unmodified DarA and distinct from that of darobactin A (Figure 2b). LC–HRMS analysis of P0 showed the molecular weight to be 2 Da smaller than that of DarA (Figure 2c). Therefore, we tentatively assigned P0 to be DarA with a single C–C crosslink, likely between W3 and K5.

Since no ether crosslink formation was reproducibly observed with His-*Pl*DarE even after extensive screening of the reaction conditions, we hypothesized that the *N*-terminal His-tag may be interfering with the DarE function. Therefore, we created an *N*-terminally Strep-tagged DarE with a Factor Xa cleavage site immediately preceding the first codon of DarE (Strep-*Pl*DarE) for a traceless tag removal. This protein was expressed in *E. coli* in a manner similar to that of His-*Pl*DarE and purified using a Strep-tactin resin. Subsequently,

the Strep-tag was cleaved by treatment with Factor Xa protease. The resulting enzyme contained 7.5 ± 0.7 equiv of Fe. Subsequent chemical reconstitution increased the Fe content to 12.2 ± 0.5 equiv per monomer, consistent with the presence of three 4Fe–4S clusters per monomer. This result is in a sharp contrast to His-*Pf*DarE, where we observed only ~9 Fe per monomer.

The resulting untagged *Pf*DarE was tested for its catalytic function using *Pf*DarA. When we investigated its activity under strictly anaerobic conditions (<0.1 ppm O_2), we observed a single product (P1, Figure 3a, trace i) with a unique UV absorption band at ~350 nm (Figure 3b). P1 was produced only in the presence of SAM, NADPH, DarE, and DarA, supporting that it is produced by the radical SAM activity of DarE. Furthermore, LC–HRMS analysis revealed its molecular weight to be 2 Da smaller than that of DarA (Figure 3c). Importantly, P1 was distinct from P0 observed in the His-*Pf*DarE reaction, and P0 was not detectable in the assays with *Pf*DarE fully loaded with three 4Fe–4S clusters.

Since we did not observe any oxygen insertion, we tested the activity of DarE in the presence of oxygen. Upon testing several assay conditions, we observed the formation of two products (Figure 3a). One of them co-migrated with P1 formed in the absence of O_2, but the other product (P2) migrated at a distinct retention time. P2 was not observed when O_2 was replaced with hydrogen peroxide or potassium superoxide (Figure S7). In the presence of O_2, the formation of P1 and P2 accompanied the production of 5′-dA (Figure S8), supporting that their production requires the reductive SAM cleavage. The UV–vis absorption spectrum of P2 was distinct from that of P1 or DarA and agreed with that of darobactin A (Figure 3b). P2 was produced only in the presence of O_2, SAM, and *Pf*DarE (Figure 3a). In addition, P2 production was observed only when flavodoxin/flavodoxin reductase was used as a reductant and not when using either SDT or Ti(III) citrate as a reductant (Figure S7). LC–MS characterization of this species revealed its molecular weight to be 12 Da larger than that of DarA (Figure 3c), which is consistent with the presence of two crosslinks and the addition of an oxygen atom.

To better characterize P1 and P2, we purified them by HPLC (Figure S9) and digested with proteinase K. Proteinase K has broad specificity and hydrolyzes amide bonds at the C-terminus to hydrophobic (aliphatic and aromatic) amino acids. The proteinase K treatment of each of these compounds yielded only one major product with UV absorption features identical to those of the parent molecules (Figure 4a,b). Based on the quantitation of the HPLC peak before and after the proteinase K treatment, the transformation was quantitative (>90% yield). Importantly, the proteinase K digest of P2 co-migrated with darobactin A on HPLC and LC–MS (Figures 4b, and S10) and showed an identical molecular weight to darobactin A (Figure 4c). Moreover, the MS/MS fragmentation pattern agreed with darobactin A (Figure S11) with the observation of the key fragment ions characteristic to the ether crosslinking, including those with hydroxyindole (Figures S11 and S12). These observations provided strong evidence that P2 has the ether and C–C crosslinks identical to that of darobactin A, and the physiological function of DarE is the C–C and ether crosslink formation using molecular oxygen as the source of ether oxygen.

The molecular weight of the P1 proteinase K digest (Figure 4c, panel i) was consistent with a pentapeptide (WNWSK) from the core sequence of DarA with a loss of 2 Da. The MS/MS fragmentation pattern was consistent with the loss of two hydrogen atoms from the W3 residue (Figures S11 and S12). No fragment ions specific to a C–C crosslink were observed, and the unique UV–vis absorption band at 350 nm suggests the presence of an extended aromatic system. Therefore, although we cannot fully eliminate the possibility of a W1–W3 C–C crosslink, we characterize P1 as DarA with Cα-Cβ desaturation of W3. To test if P1 is an intermediate of the P2 formation, we incubated purified P1 with DarE. However, even after prolonged incubation (>10 h), P1 was not consumed, and no products, including P2, were observed. Based on this observation, we propose P1 as an off-pathway shunt product.

To obtain further evidence for the use of O_2 as the source of ether oxygen, we performed the *Pl*DarE assay in the presence of $^{18}O_2$. The MS characterization of P2 formed in the presence of $^{18}O_2$ suggested an increase of the molecular weight by 2 Da compared to that of P2 from the assay with natural isotope O_2 (Figure 5a). Based on the isotope signal pattern, the ^{18}O enrichment of P2 generated in the presence of $^{18}O_2$ was calculated as 81 ± 2% (Figure S13), which likely represents the imperfect $^{18}O_2$ replacement. Furthermore, when we converted P2 produced in $^{18}O_2$ into darobactin A, we observed a 2 Da increase of the molecular weight of darobactin A (Figure 5b). The ^{18}O enrichment in darobactin A was estimated to be 85 ± 3% based on the ratio of the MS signal intensities at *m/z* 483.71 and 484.71 $[M + 2H]^{2+}$. To test if ^{18}O in water is incorporated into P2, we performed the DarE assay in [^{18}O]water (80% enrichment) with natural isotope O_2. The resulting P2 and its proteinase K digest exhibited mass spectra indistinguishable from those of P2 formed in natural isotope water (Figure 5a,b). The comparison of the *m/z* 483.71 and 484.71 signal intensities in the proteinase K digest revealed no detectable level of ^{18}O incorporation (<5%, Figure 5b). These observations together suggest that DarE incorporates one of the oxygen atoms of O_2 into the ether crosslink of P2. In sum, these results demonstrate that DarE catalyzes both C–C and ether crosslinking during darobactin A biosynthesis using O_2 as a native co-substrate.

To obtain mechanistic insights into the DarE catalysis, we determined the stoichiometry of the reaction. P1 was quantified using synthetic darobactin core heptapeptide (WNWSKSF) as a standard. P2 was quantified using darobactin A as a standard. The extinction coefficient of darobactin A was determined to be 2.9 cm^{-1} mM^{-1} at 280 nm, which was significantly less than that of unmodified *Pl*DarA (11.2 cm^{-1} mM^{-1}), suggesting the significant effects of the indole ring modifications on the light absorption feature. Using these standards, HPLC quantitation revealed the formation of 10.8 ± 2.9 μM P1 and 50.3 ± 8.7 μM P2 from 100 μM *Pl*DarA, suggesting that P2 is the major product of *Pl*DarE assays. In the same assays, 5′-dA was quantified by HPLC as 111 ± 15 μM. Thus, the ratio of P1 : P2 : 5′-dA was 0.21 ± 0.04 : 1.0 : 2.3 ± 0.5. Since the desaturation reaction likely consumes 1 equiv of SAM, the results suggest that DarE consumes 2 equiv of SAM to produce P2.

Finally, we performed the activity assays using substoichiometric amounts of *Pl*DarE relative to *Pl*DarA. Consequently, we found that, at least under the current assay conditions, the amounts of P1 and P2 were always substoichiometric to *PlDarE* (Figure S7a). Since *Pl*DarE catalyzes both the ether and C–C crosslinking without detectable accumulation of

intermediates, *Pl*DarE is likely catalytic. Thus, the substoichiometric product formation is most likely due to a strong product inhibition, and a product release may require proteolytic cleavage of the leader peptide.

DISCUSSION

Our characterization of *Pl*DarE revealed that this enzyme catalyzes both the ether and C–C crosslinks and produces modified DarA (P2) that can be converted into darobactin A after digestion with proteinase K. Of particular significance, we found that *Pl*DarE uses O_2 as the source of ether bond oxygen. This result is in sharp contrast to the recent proposal that *N*-terminally His-tagged *P. khanii* DarE (His-*Pk*DarE) incorporates ^{18}O from water into its product (DarA with a 14 Da modification). Although we cannot eliminate the possibility that *Pl*DarE and *Pk*DarE (61% amino acid sequence identity) catalyze the ether crosslinking in two distinct mechanisms, the reported characterization of the His-*Pk*DarE product leaves significant ambiguity. The structure was proposed solely based on MS without showing specific fragment ions for the ether crosslink. The authors did not describe if the DarA + 14 Da species can be converted to darobactin A. No results were reported for His-*Pk*DarE assays in the presence of O_2. In addition, the His-*Pk*DarE was partially reconstituted with only 8 Fe/DarE. Therefore, further characterizations are required to make conclusions about the mechanism of ether crosslink formation by *Pk*DarE.

Still, the comparison of the results between His-*Pk*DarE and His-*Pl*DarE assays revealed an important commonality. In both cases, the major product is missing either or both of the ether and/or C–C crosslinks. His-*Pk*DarE produced *Pk*DarA +14 Da species as the major product and His-*Pl*DarE produced *Pl*DarA – 2 Da (P0). Even when the His-*Pl*DarE assays were performed in the presence of O_2, P0 remained the major product (Figure 2c). Importantly, both His-*Pk*DarE and His-*Pl*DarE were loaded with only 8–9 Fe per monomer. On the other hand, the untagged *Pl*DarE was fully loaded with 12 Fe per monomer, suggesting the successful assembly of all three 4Fe–4S clusters. Therefore, the observed functional difference between His-tagged and untagged DarE is likely caused by the amount of cluster loading.

The ability of DarE to use O_2 as a co-substrate in the physiologically relevant reaction is unprecedented among radical SAM enzymes. The only reported example of a radical SAM enzyme reaction with O_2 is for MqnE,[16] where the reaction with a substrate analogue designed to trap a radical intermediate yielded a hydroperoxide adduct. However, MqnE does not catalyze such a reaction with the native substrate and is hence unlikely to possess a specific mechanism to catalyze the hydroperoxide addition reaction. Thus, DarE's native oxygenase activity is unprecedented and is of significant mechanistic interest.

Scheme 1 summarizes the possible mechanisms of O_2-dependent ether crosslinking by DarE. Our current favorite mechanism is a reaction of O_2 with the W3 Cβ radical (mechanism A). In this mechanism, DarE abstracts the Hβ atom of W3 and the resulting radical adds to O_2. Subsequent transfers of an electron and a proton would yield a hydroperoxide intermediate. This reaction is analogous to that of the MqnE reaction with the radical-trapping substrate analogue. In the MqnE reaction, the stabilization of the organic

radical using the substrate was critical for its reaction with O_2. In the DarE catalysis, the W3 Cβ radical is stabilized by the delocalization through the indole ring, which may allow O_2 to react. For the subsequent ether formation, multiple mechanisms are conceivable. For example, a nucleophilic attack of the indole ring of W1 to the hydroperoxide followed by rearomatization would yield the ether product (mechanism A1). Alternatively, a transfer of an electron and a proton would allow homolytic cleavage of the O–O bond to yield an alkoxy radical, which then attacks the indole ring of W1 (Scheme 1, mechanism A2). Subsequent oxidative quenching of the indole radical would yield the ether product.

The observation of P1 as a minor shunt product is also consistent with the formation of the W3 Cβ radical. Most likely, P1 is formed when the W3 Cβ radical is formed in the absence of O_2 bound to the active site, or the AUX clusters are in the incorrect redox state. (Note: the production of P1 requires an electron acceptor, whereas the ether crosslinking requires an electron donor.) Thus, the proposed mechanism explains the P1 formation in the absence of O_2 or redox mismatch (see below for the relationship between the reductant and AUX clusters). Since P1 was not converted to the ether product, we can eliminate all the mechanistic options with P1 as an intermediate including the one proposed by Guo et al.[12]

Tryptophan is susceptible to oxidation by reactive oxygen species (ROS),[17] and 7-hydroxylation proceeds by the addition of a hydroxyl radical.[17,18] Thus, it is also conceivable that the oxygen insertion by DarE proceeds via W1 oxidation using ROS such as the hydroxyl radical generated from O_2 in the active site (Scheme 1, mechanism B). The resulting 7-hydroxy-W1 would be used for ether bond formation using a radical SAM chemistry either via coordination of the 7-hydroxy group to the AUX1 cluster or α,β-desaturated W3 in a way similar to what has been proposed for thioether crosslinked RiPP biosynthesis.[10,19,20] In this mechanism, the P1 formation is explained by a promiscuous reactivity of DarE, in which DarE generates the W3-Cβ radical prior to the W1 oxidation. To test mechanism B, we performed DarE assays with hydrogen peroxide or potassium superoxide, potential precursors of hydroxyl radical formation from O_2. However, no P2 was observed. No W1 oxidation was observed when the DarE assays were performed in the absence of SAM. Thus, while these results do not necessarily eliminate mechanism B, we currently think it is less likely.

In our in vitro assays, the ether crosslink was observed only when flavodoxin was used as a reductant. Assays with chemical reductants, such as SDT or Ti(III) citrate, did not yield P2. The observed requirement for flavodoxin is likely due to the rapid scavenging of oxygen by chemical reductants (e.g., ~700 μM s^{-1} with 2 mM SDT at 25 °C[21]) compared to flavodoxin (~0.0017 μM s^{-1}[22]). In addition, flavodoxin may be able to better set the redox state of the 4Fe–4S clusters for the ether bond formation. The proposed mechanisms of ether crosslinking require an injection of at least one electron (Scheme 1). While the donor of this electron is currently unknown, one of the candidates is the AUX clusters. On the other hand, the formation of C–C crosslinking between W3 and K5 would require the AUX clusters to serve as electron acceptors (see Scheme 2 and the related discussion below). Therefore, the AUX clusters of DarE would serve as both the electron donor and acceptor, in which the AUX clusters must be in an appropriate redox state in each step of catalysis without being over-reduced or oxidized. Such an adjustment may be better achieved by a

more physiologically relevant reductant, flavodoxin, than by chemical reductants. In general, the role of reductase in radical SAM enzymes is not well-understood, although biological reductases were reported to be critical for the physiological function of several radical SAM enzymes, including PqqE[23] and NosL.[24] Our observation of the strict requirement of flavodoxin for DarE's oxygenase activity further emphasizes the significant role of reductases in radical SAM enzyme catalysis.

DarE's use of O_2 as a co-substrate in the biologically relevant reaction is unprecedented in radical SAM enzymes and was unexpected due to the oxygen-sensitive nature of radical SAM enzymes. However, accumulating evidence suggests that radical SAM enzymes function in aerobic cells. A recent study of Dph1–Dph2 suggested that this non-canonical radical SAM enzyme in diphthamide biosynthesis is associated with an Fe-protein Dph3 that can donate Fe and repair an oxidatively damaged 4Fe–4S cluster of Dph1–Dph2.[25] While the mechanism of cluster maintenance and the physiological reductase are unknown for most other radical SAM enzymes, the presence of such mechanisms in cells would allow radical SAM enzymes to function under aerobic conditions. Our discovery of DarE as a radical SAM oxygenase emphasizes that at least some radical SAM enzymes function under an aerobic cellular environment and can tolerate certain levels of O_2 in the presence of the physiological reductant or 4Fe–4S cluster maintenance machinery.

In addition to the ether crosslink, DarE catalyzed the C–C crosslinking between W3 and K5. A recent report on SuiB,[26] a radical SAM enzyme that catalyzes C–C crosslinking during the biosynthesis of streptide RiPPs, suggested that the C–C bond crosslinking on these RiPPs proceeds through the formation of an amino acid Cβ radical, followed by its addition to an sp^2 carbon of an aromatic side chain and oxidative radical quenching.[27] This mechanism is certainly a plausible option for DarE's W3–K5 crosslinking. However, considering the distant sequence similarity of DarE and SuiB, it is also possible that DarE catalyzes the C–C crosslinking by a different mechanism. Thus, we here consider an alternative mechanism, in which the K5 Cβ radical is oxidatively quenched to yield an α,β-unsaturated peptide (Scheme 2, mechanism B). The subsequent nucleophilic attack of W3 would yield the C–C crosslink. The nucleophilic mechanism was originally proposed for radical SAM enzymes that form thioether crosslinked RiPPs,[19] although limited evidence is currently available. For DarE, our observation of P1 production is consistent with DarE's ability to catalyze the α,β-desaturation. Further study is needed to test if the α,β-desaturation is used as a mechanism of the C–C crosslink formation.

The order of C–C and ether crosslink formation may be deduced from our current observations. The formation of P1 demonstrates that DarE can generate the Cβ radical on W3 without the W3–K5 crosslinking. No W3–K5 crosslink was observed in the absence of the W1–W3 crosslink. Thus, although we cannot be exclusive, our data suggest that the W1–W3 ether crosslink precedes the W3–K5 crosslink. Future characterization of an on-pathway intermediate will provide further insights into the order of crosslink formation.

CONCLUSIONS

Our in vitro characterization of *Pl*DarE elucidated that this enzyme is a unique dual-function enzyme that catalyzes both the ether and C–C crosslinks. The ether crosslink formation requires O_2 as the source of the ether oxygen. *Pl*DarE also catalyzed the production of an α,β-unsaturated peptide. Thus, this enzyme makes three chemically distinct modifications on the DarA peptide substrate. Future mechanistic characterization of this enzyme would reveal novel insights into the mechanism of RiPP biosynthesis by radical SAM enzymes.

Supplementary Material

Refer to Web version on PubMed Central for supplementary material.

ACKNOWLEDGMENTS

We acknowledge Leo Padva for cloning initial expression constructs and thank Yu Imai for providing darobactin A.

Funding

This work was supported by the Duke University School of Medicine and in part the National Institute of General Medical Sciences R01 GM112838 (to K.Y.) and by the National Institute of Allergy and Infectious Diseases R01 AI158388 (to K.L.). I Dewa M. Kresna thanks the Deutscher Akademischer Austauschdienst (DAAD) for his PhD scholarship. The German Federal Ministry of Education and Research (BMBF) and the Hesse State Ministry of Higher Education Research and Arts (HMWK) supported research in the Schaberle lab. J.R., E.d.l.M., and Y.N thank the French National Research agency for financial support through the contract ANR-20-CE44-0005. They used the platforms of the Grenoble Instruct-ERIC center (ISBG; UMS 3518 CNRS-CEA-UGA-EMBL) within the Grenoble Partnership for Structural Biology (PSB), which is supported by FRISBI (ANR-10-INBS-05-02) and GRAL and financed within the Universite Grenoble Alpes graduate school (Ecoles Universitaires de Recherche) CBH-EUR-GS (ANR-17-EURE-0003).

ABBREVIATIONS

BGC	biosynthetic gene cluster
RiPP	ribosomally synthesized and post-translationally modified peptide
SAM	*S*-adenosylmethionine
AA	amino acid

REFERENCES

(1). Imai Y; Meyer KJ; Iinishi A; Favre-Godal Q; Green R; Manuse S; Caboni M; Mori M; Niles S; Ghiglieri M; et al. A new antibiotic selectively kills Gram-negative pathogens (vol 576, pg 459, 2019). Nature 2020, 580, No. E3. [PubMed: 32269338]

(2). Kaur H; Jakob RP; Marzinek JK; Green R; Imai Y; Bolla JR; Agustoni E; Robinson CV; Bond PJ; Lewis K; et al. The antibiotic darobactin mimics a beta-strand to inhibit outer membrane insertase. Nature 2021, 593, 125. [PubMed: 33854236]

(3). Wuisan ZG; Kresna IDM; Böhringer N; Lewis K; Schäberle TF Optimization of heterologous Darobactin A expression and identification of the minimal biosynthetic gene cluster. Metab. Eng 2021, 66, 123–136. [PubMed: 33872780]

(4). Groß S; Panter F; Pogorevc D; Seyfert CE; Deckarm S; Bader CD; Herrmann J; Müller R Improved broad-spectrum antibiotics against Gram-negative pathogens via darobactin biosynthetic pathway engineering. Chem. Sci 2021, 12, 11882–11893. [PubMed: 34659729]

(5). Sofia HJ; Chen G; Hetzler BG; Reyes-Spindola JF; Miller NE Radical SAM, a novel protein superfamily linking unresolved steps in familiar biosynthetic pathways with radical mechanisms: functional characterization using new analysis and information visualization methods. Nucleic Acids Res. 2001, 29, 1097–1106. [PubMed: 11222759]

(6). Broderick JB; Duffus BR; Duschene KS; Shepard EM Radical S-adenosylmethionine enzymes. Chem. Rev 2014, 114, 4229–4317 Research Support, N.I.H., Extramural Research Support, U.S. Gov't, Non-P.H.S.. [PubMed: 24476342]

(7). Grell TA; Goldman PJ; Drennan CL SPASM and twitch domains in S-adenosylmethionine (SAM) radical enzymes. J. Biol. Chem 2015, 290, 3964–3971. [PubMed: 25477505]

(8). Schramma KR; Bushin LB; Seyedsayamdost MR Structure and biosynthesis of a macrocyclic peptide containing an unprecedented lysine-to-tryptophan crosslink. Nat. Chem 2015, 7, 431–437. [PubMed: 25901822]

(9). Nguyen TQN; Tooh YW; Sugiyama R; Nguyen TPD; Purushothaman M; Leow L; Hanif K; Yong RHS; Agatha I; Winnerdy FR; et al. Post-translational formation of strained cyclophanes in bacteria. Nat. Chem 2020, 12, 1042. [PubMed: 32807886]

(10). Flühe L; Knappe TA; Gattner MJ; Schäfer A; Burghaus O; Linne U; Marahiel MA The radical SAM enzyme AlbA catalyzes thioether bond formation in subtilosin A (vol 8, pg 350, 2012). Nat. Chem. Biol 2012, 8, 737.

(11). Clark KA; Bushin LB; Seyedsayamdost MR Aliphatic Ether Bond Formation Expands the Scope of Radical SAM Enzymes in Natural Product Biosynthesis. J. Am. Chem. Soc 2019, 141, 10610–10615. [PubMed: 31246011]

(12). Guo S; Wang S; Ma S; Deng Z; Ding W; Zhang Q Radical SAM-dependent ether crosslink in daropeptide biosynthesis. Nat. Commun 2022, 13, 2361. [PubMed: 35487921]

(13). Grote A; Hiller K; Scheer M; Munch R; Nortemann B; Hempel DC; Jahn D JCat: a novel tool to adapt codon usage of a target gene to its potential expression host. Nucleic Acids Res. 2005, 33, W526–W531. [PubMed: 15980527]

(14). Gibson DG; Young L; Chuang R-Y; Venter JC; Hutchison CA; Smith HO Enzymatic assembly of DNA molecules up to several hundred kilobases. Nat. Methods 2009, 6, 343–345. [PubMed: 19363495]

(15). fish WW Rapid Colorimetric Micromethod for the Quantitation of Complexed Iron in Biological Samples. Methods Enzymol. 1988, 158, 357–364. [PubMed: 3374387]

(16). Joshi S; Fedoseyenko D; Sharma V; Nesbit MA; Britt RD; Begley TP Menaquinone Biosynthesis: New Strategies to Trap Radical Intermediates in the MqnE-Catalyzed Reaction. Biochemistry 2021, 60, 1642–1646. [PubMed: 33999605]

(17). Jacobitz AW; Liu Q; Suravajjala S; Agrawal NJ Tryptophan Oxidation of a Monoclonal Antibody Under Diverse Oxidative Stress Conditions: Distinct Oxidative Pathways Favor Specific Tryptophan Residues. J. Pharm. Sci 2021, 110, 719–726. [PubMed: 33198947]

(18). Solar S; Solar W; Getoff N Resolved Multisite Oh-Attack on Aqueous Tryptophan Studied by Pulse-Radiolysis. Radiat. Phys. Chem 1984, 23, 371–376.

(19). Bruender NA; Wilcoxen J; Britt RD; Bandarian V Biochemical and Spectroscopic Characterization of a Radical S-Adenosyl-L-methionine Enzyme Involved in the Formation of a Peptide Thioether Cross-Link. Biochemistry 2016, 55, 2122–2134. [PubMed: 27007615]

(20). Grove TL; Himes PM; Hwang S; Yumerefendi H; Bonanno JB; Kuhlman B; Almo SC; Bowers AA Structural Insights into Thioether Bond Formation in the Biosynthesis of Sactipeptides. J. Am. Chem. Soc 2017, 139, 11734–11744. [PubMed: 28704043]

(21). Tao Z; Goodisman J; Souid AK Oxygen measurement via phosphorescence: reaction of sodium dithionite with dissolved oxygen. J. Phys. Chem. A 2008, 112, 1511–1518. [PubMed: 18229902]

(22). Mayhew SG; Foust GP; Massey V Oxidation-reduction properties of flavodoxin from Peptostreptococcus elsdenii. J. Biol. Chem 1969, 244, 803–810. [PubMed: 4388813]

(23). Barr I; Latham JA; Iavarone AT; Chantarojsiri T; Hwang JD; Klinman JP Demonstration That the Radical S-Adenosylmethionine (SAM) Enzyme PqqE Catalyzes de Novo Carbon-Carbon Cross-linking within a Peptide Substrate PqqA in the Presence of the Peptide Chaperone PqqD. J. Biol. Chem 2016, 291, 8877–8884. [PubMed: 26961875]

(24). Sicoli G; Mouesca JM; Zeppieri L; Amara P; Martin L; Barra AL; Fontecilla-Camps JC; Gambarelli S; Nicolet Y Fine-tuning of a radical-based reaction by radical S-adenosyl-L-methionine tryptophan lyase. Science 2016, 351, 1320–1323. [PubMed: 26989252]

(25). Zhang YG; Su D; Dzikovski B; Majer SH; Coleman R; Chandrasekaran S; Fenwick MK; Crane BR; Lancaster KM; Freed JH; et al. Dph3 Enables Aerobic Diphthamide Biosynthesis by Donating One Iron Atom to Transform a [3Fe-4S] to a [4Fe-4S] Cluster in Dph1-Dph2. J. Am. Chem. Soc 2021, 143, 9314–9319. [PubMed: 34154323]

(26). Balo AR; Caruso A; Tao L; Tantillo DJ; Seyedsayamdost MR; Britt RD Trapping a cross-linked lysinetryptophan radical in the catalytic cycle of the radical SAM enzyme SuiB. Proc. Natl. Acad. Sci. U.S.A 2021, 118, No. e2101571118.

(27). Yokoyama K; Lilla EA C-C bond forming radical SAM enzymes involved in the construction of carbon skeletons of cofactors and natural products. Nat. Prod. Rep 2018, 35, 660–694. [PubMed: 29633774]

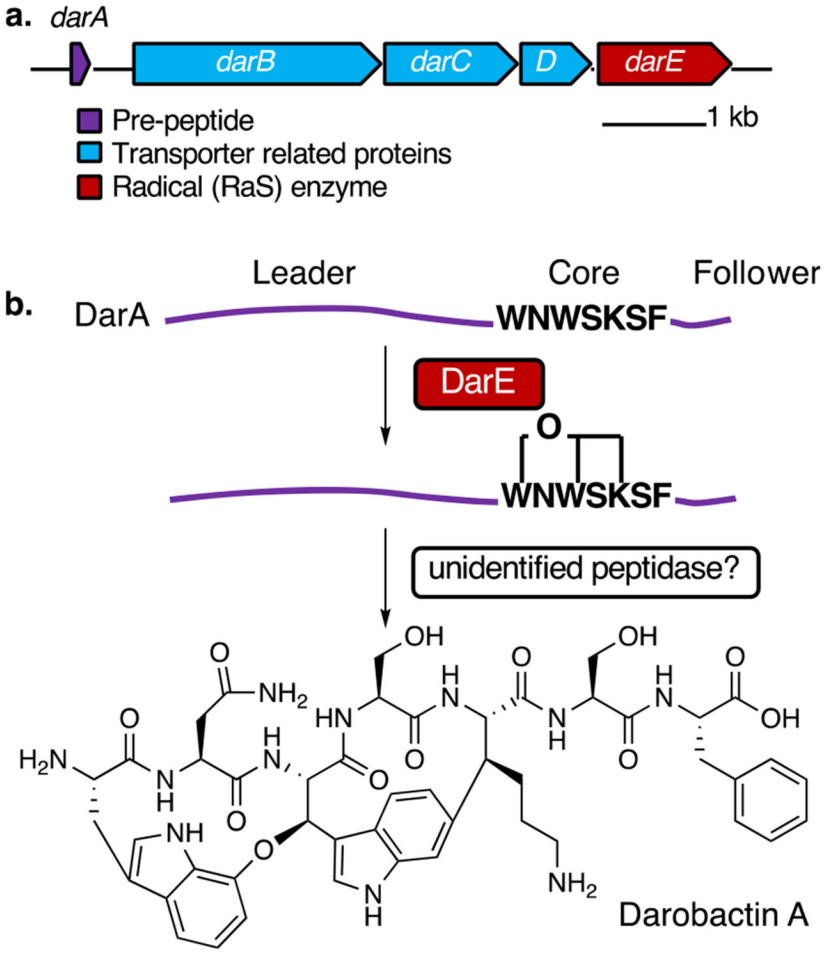

Figure 1.
Darobactin A biosynthesis. (a) BGC of darobactin A. (b) Proposed biosynthetic pathway of darobactin A.

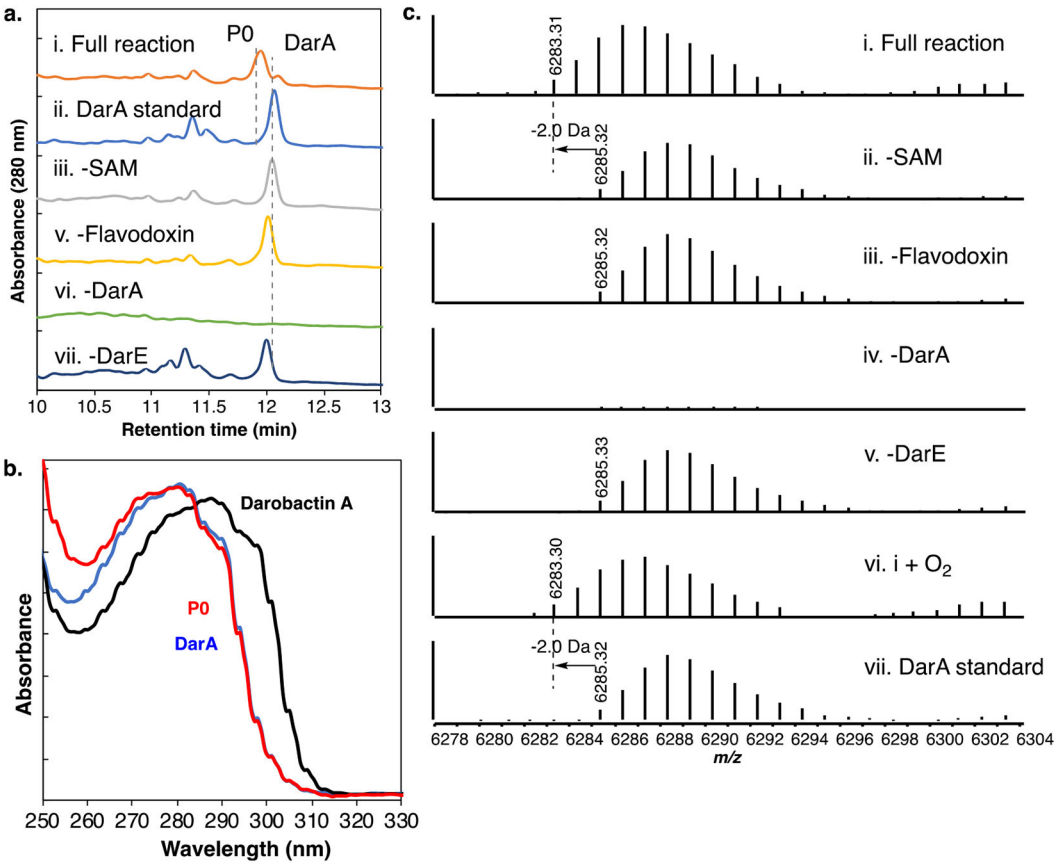

Figure 2.

Characterization of His-*Pl*DarE. (a) HPLC characterization of His-DarE assays. (b) UV–vis spectra of P0, DarA, and darobactin A. (c) Extracted and deconvoluted mass spectra of His-*Pl*DarE assays. Mass spectra were extracted from the retention time that covers unmodified *Pl*DarA and P0.

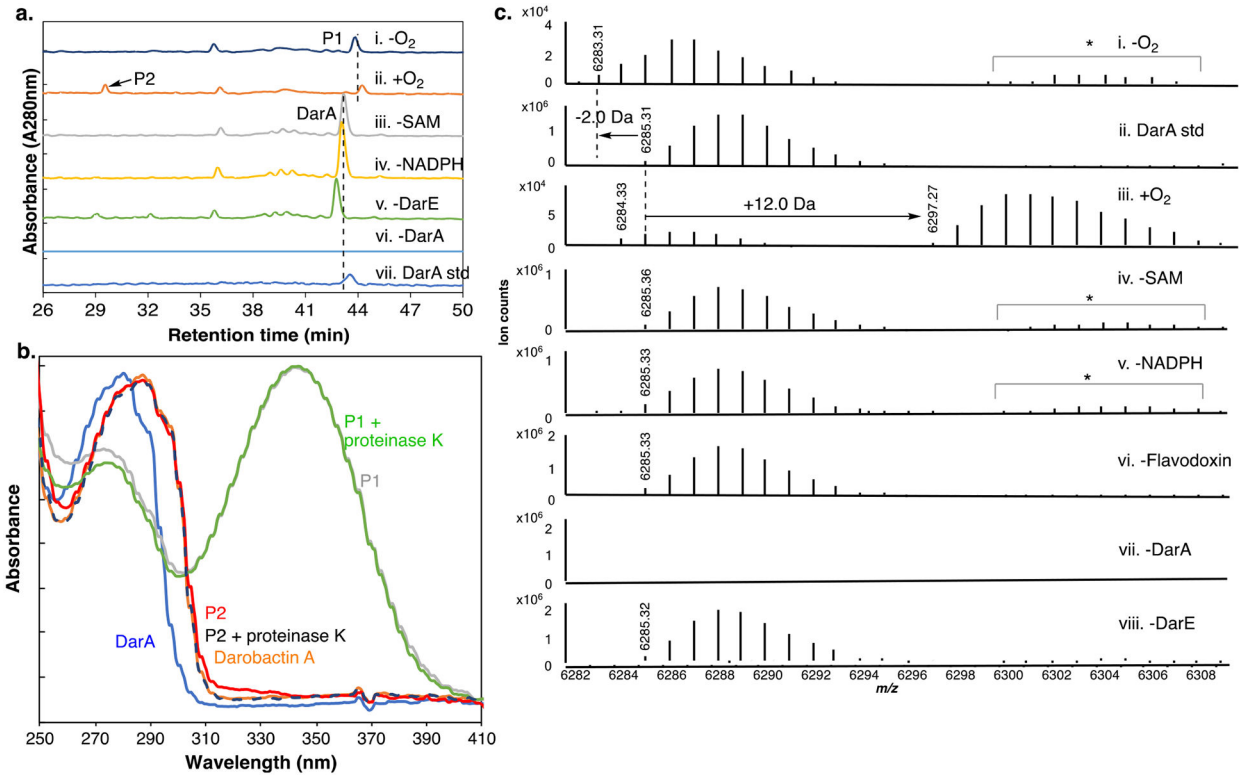

Figure 3.

Activity assays of *Pl*DarE. (a) HPLC analyses of *Pl*DarE assay in the absence of O_2 (i), in the presence of O_2 (ii), (ii) without SAM (iii), (ii) without NADPH (iv), (ii) without *Pl*DarE (v), (ii) without *Pl*DarA (vi), and the *Pl*DarA standard (vii). (b) UV–vis absorption spectra of P1 (gray), P1 + proteinase K (green), P2 (red), P2 + proteinase K (dashed black), darobactin A (orange), and *Pl*DarA (blue). (c) Extracted and deconvoluted mass spectra of DarE assays. Mass spectra were extracted from the retention time that covers unmodified *Pl*DarA, P1, and P2. The mass peaks indicated with asterisks (*) have a molecular weight close to that of *Pl*DarA with a 14 Da modification, but they were also present in the controls without SAM or NADPH and hence unlikely to be the product of the radical SAM enzyme activity.

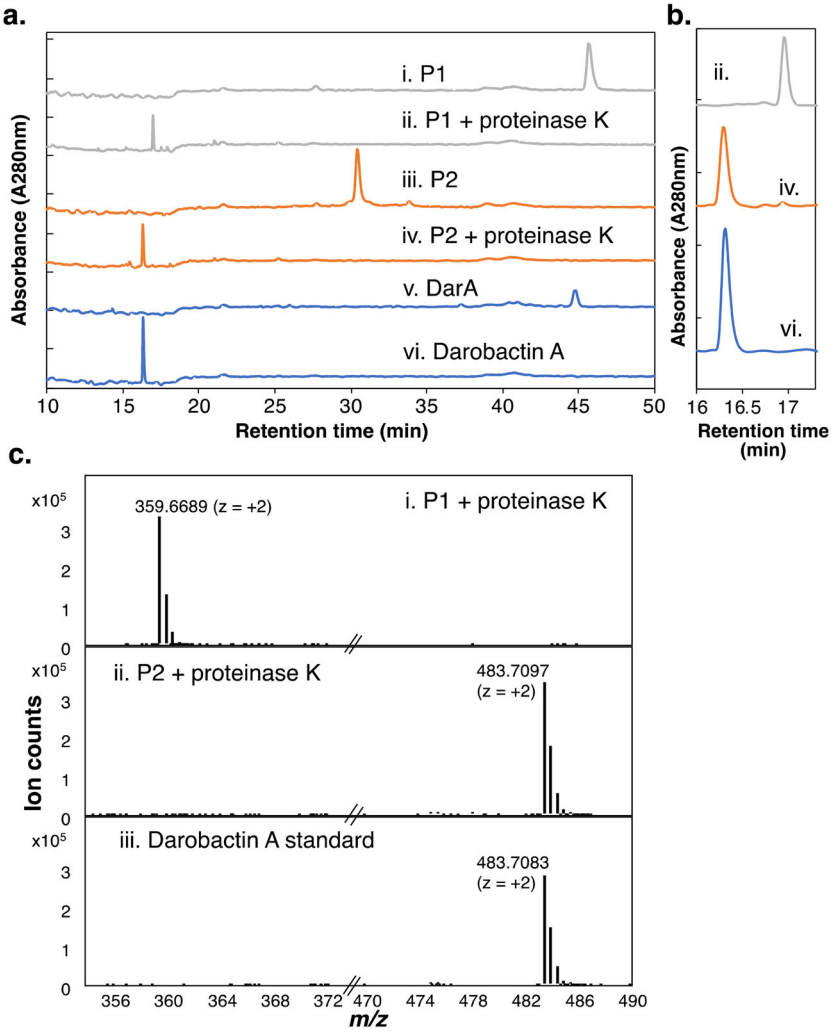

Figure 4.

Characterization of *Pl*DarE products. Shown are HPLC chromatograms (a and b) and mass spectra (c) of P1, P2, P1 + proteinase K, P2 + proteinase K, and the darobactin A standard. (b) magnified view of (ii), (iv), and (vi) in (a). See Figure S10 for the extracted ion chromatograms and full-range MS spectra.

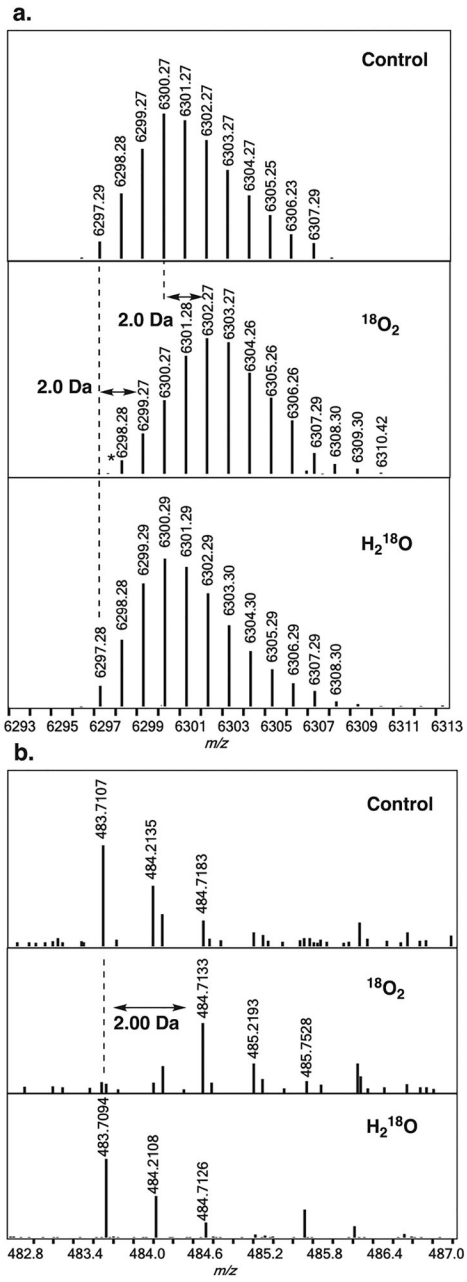

Figure 5.

Characterization of P2 formed in the presence of $^{18}O_2$ or [^{18}O]water. (a) Mass spectra of P2 formed in the presence of natural isotope O_2, $^{18}O_2$, or [^{18}O]water. (b) Mass spectra of proteinase K digests of P2 formed in the presence of natural isotope O_2, $^{18}O_2$, or [^{18}O]water. Shown are the z = +2 ions. Calculated *m/z* for [^{18}O]darobactin A = 484.7110 $[M + 2H]^{2+}$; Observed *m/z* 484.7133 (4.8 ppm). Calculated *m/z* for darobactin A = 483.7089 $[M + 2H]^{2+}$; Observed *m/z* 483.7107 (3.7 ppm) and 483.7094 (1.0 ppm). * indicates the presence of natural abundance isotope P2 due to the imperfect $[^{18}O_2]O_2$ gas exchange (see Figure S13 for the calculation of the ^{18}O enrichment).

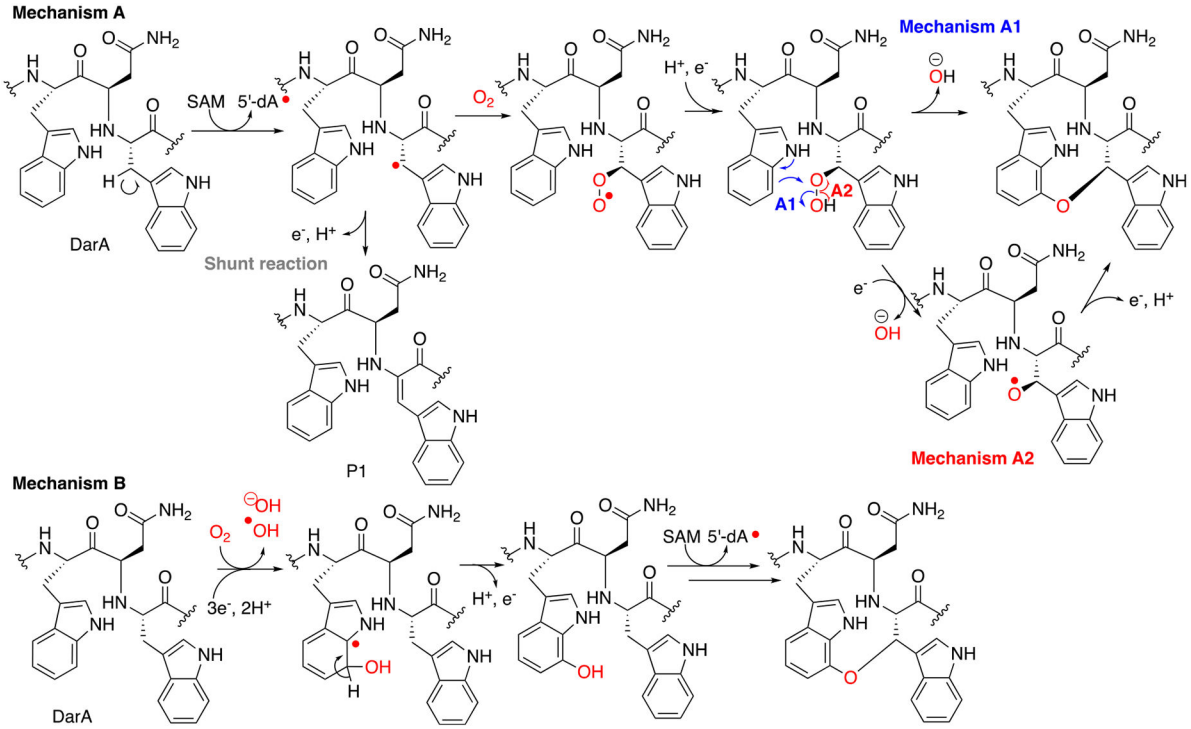

Scheme 1.
Proposed Mechanisms of DarE-catalyzed Ether Crosslink Formation

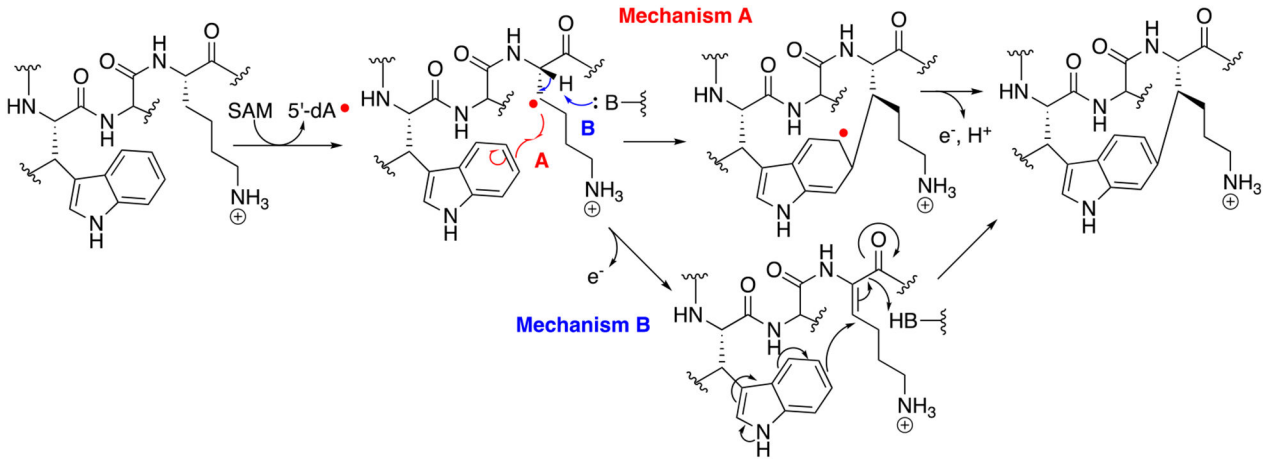

Scheme 2.

Proposed Mechanisms of DarE-catalyzed C–C Crosslink Formation